Crystallization mechanisms for supercooled liquid Xe at high pressure and temperature: Hybrid Monte Carlo molecular simulations

Caroline Desgranges and Jerome Delhommelle
Department of Chemical Engineering, 301 Main Street, University of South Carolina, Columbia, South Carolina 29208, USA
(Received 21 June 2007; revised manuscript received 24 December 2007; published 15 February 2008)

We report hybrid Monte Carlo molecular simulation results on the crystallization of supercooled liquids of xenon at high temperature and high pressure. We simulate the entire crystallization process, i.e., the nucleation event as well as the subsequent growth of the critical nucleus, at $P=4.46$ GPa and $P=87.96$ GPa. In both cases, we carry out the simulations at a temperature 25% below the melting temperature. We demonstrate that the crystallization mechanism strongly depends on pressure. At $P=4.46$ GPa, crystal nucleation and growth both proceed through the face centered cubic (fcc) polymorph. At $P=87.96$ GPa, throughout nucleation and growth, the crystallites are always predominantly of the body centered cubic (bcc) form. However, at $P=87.96$ GPa, our simulations reveal that the crystallization mechanism is rather complex. Precritical as well as large postcritical crystallites can often be described as composed of several blocks: a large block of the thermodynamically stable bcc polymorph and smaller metastable fcc blocks, which gradually convert into the stable bcc form. We rationalize these results in terms of the relative stability of the phases involved and compare the crystallization mechanism of xenon to those recently observed on model systems.

DOI: 10.1103/PhysRevB.77.054201 PACS number(s): 61.50.Ks, 64.70.D−, 61.20.Ja, 81.10.Aj

I. INTRODUCTION

Polymorphism is the ability of an atom or a molecule to crystallize in different structures or polymorphs.[1,2] Since each polymorph has specific physical properties, it is crucial to control which polymorphs form during the crystallization process. This raises the issue of understanding which, when, and how polymorphs will be formed during the crystallization process. This is a very complex problem, resulting from a subtle interplay between thermodynamics and kinetics. Solving this issue has remained elusive so far, even on simple model systems such as the Lennard-Jones fluid or charge-stabilized colloidal suspensions modeled by the Yukawa potential. Recent simulations on the crystallization of the Lennard-Jones fluid from the supercooled liquid have shed light on this phenomenon[3–5,7,6] by demonstrating how thermodynamic conditions of crystallization dramatically influence the polymorph selection process. At low pressure,[3,5] crystal nucleation proceeds first into the metastable body centered cubic (bcc) phase and then into the thermodynamically stable face centered cubic (fcc) phase. Subsequent growth of the critical nucleus gives rise to the cross nucleation (or heterogeneous nucleation) of another metastable form, the hexagonal close packed (hcp) structure, on the structurally compatible (111) planes of the predominantly fcc nucleus. At high pressure, both crystal nucleation and growth proceed into the metastable bcc form.[7] Fine tuning the value of the applied pressure at fixed supercooling or the amount of supercooling at fixed pressure allows us to control the fraction of the fcc and bcc forms in the crystallite as well as the amount of cross nucleation. Similarly, recent simulations have shed light on the crystallization mechanisms of charge-stabilized colloidal suspensions modeled by the Yukawa potential.[8,9] By varying the value taken by the screening parameter (i.e., mimicking the addition of salt to the colloidal suspension in experiments), we were able to study the crystallization process in the domain of stability either of the fcc phase or of the bcc phase and to highlight the differences between the crystallization mechanisms for each thermodynamic condition.

In this work, we use molecular simulation to study the crystal nucleation and growth of xenon from the supercooled liquid at high pressure and high temperature. From a technological standpoint, xenon is used in many applications, e.g., as a general anesthetic[10] and in bubble chambers.[11] Studying crystallization under high pressure and high temperature also allows us to understand how this phenomenon takes place in very dense systems, e.g., subjected to Earth's core conditions. Xenon isotope ratios are, for instance, measured in meteorites to study the formation of the system solar.[12] While the Lennard-Jones potential is often thought to accurately describe the thermodynamic properties of rare gas, this is only the case under ambient conditions. In particular, an exponential law is a more adequate representation of short-range interatomic repulsion than the power law used in the Lennard-Jones form. This is especially relevant in studies of crystallization under high temperature and high pressure conditions. Under such conditions, the Buckingham[13] or exp-6 potential accurately models the interactions between Xe atoms.[14] The smoother and more realistic repulsive part of the Buckingham potential also has a dramatic effect on the phase diagram of xenon as well as on the relative stabilities of the polymorphs of xenon. The phase diagram of xenon exhibits a triple point between the fcc polymorph, the bcc polymorph, and the liquid.[15,16] In other words, the phase diagram of xenon exhibits a domain in which the bcc phase is the thermodynamically stable polymorph (see Fig. 1), unlike the phase diagram of the Lennard-Jones system (but as well as, e.g., that obtained for the inverse-power law potential with an exponent larger than 6.67).[17]

Using hybrid Monte Carlo simulations, we study how polymorph selection takes place during the crystallization of xenon for two different pressures: $P=4.46$ GPa (for which fcc is the stable crystalline form at the solid-liquid transition)

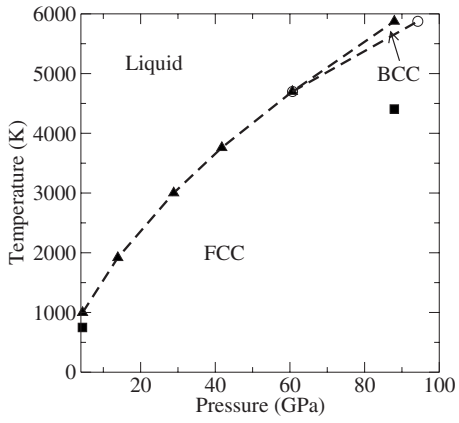

FIG. 1. High temperature–high pressure phase diagram for xenon. The triangles and circles indicate the coexistence data for the liquid-solid and the bcc-fcc transitions (Ref. 15). The squares indicate the two conditions of crystallization studied in this work.

and $P=87.96$ GPa (for which bcc is the stable crystalline form at the solid-liquid transition). In both cases, we carry out simulations of the crystallization process at a supercooling of 25%, i.e., at a temperature 25% below the melting temperature. The degree of supercooling may affect the polymorph selection process. Controlling polymorphism is essentially impossible for supercoolings larger than 30% (Ref. 4) as the free energy barriers of nucleation of all polymorphs vanish. In some systems as, e.g., in our previous work on the Lennard-Jones system,[7] carrying out the crystallization at a supercooling of 25% may yield large postcritical crystallites of the metastable form. In such cases, decreasing the supercooling (i.e., carrying out the crystallization outside the domain of occurrence of the metastable form) yields postcritical crystallites of the stable form. As shown in this work, carrying out the crystallization of xenon at a supercooling of 25% directly yields large postcritical nuclei of the stable polymorph, either the fcc form below the fcc-bcc-liquid triple point or bcc otherwise. The two sets of conditions of crystallization are plotted on the phase diagram of xenon, as shown in Fig. 1. At $P=4.46$ GPa, we show that crystallization proceeds though the fcc form with hcp-like and bcc-like atoms scattered on the surface of the crystallite. However, the crystallization mechanism is rather complex at $P=87.96$ GPa. Precritical as well as large postcritical crystallites can often be described as composed of several blocks: a large block of the thermodynamically stable bcc polymorph and smaller metastable fcc blocks, which gradually convert into the stable bcc form. We rationalize these results in terms of the relative stability of the phases involved and compare the crystallization mechanism of xenon to those recently observed on model systems. The paper is organized as follows. In the next section, we detail the numerical methods used to simulate the nucleation and growth steps of the crystallization process. We then present our results and interpret these results in terms of the relative stability of the various phases involved. We compare the crystallization mechanisms of xenon to those recently reported for model systems, such as the Lennard-Jones fluid and the colloidal suspensions modeled by the Yukawa pair potential, and finally draw the main conclusions from this work.

II. SIMULATION METHODS

We use a modified Buckingham potential (or exp-6 potential) to model the interactions between the particles of xenon at high temperature and high pressure. The potential is defined as follows:

$$U(r)=\epsilon\left\{\frac{6}{\alpha-6}\exp\left[\alpha\left(1-\frac{r}{r_m}\right)\right]-\frac{\alpha}{\alpha-6}\left(\frac{r_m}{r}\right)^6\right\}, \quad (1)$$

where α controls the softness of the repulsion and ϵ is the depth of the potential minimum located at r_m. A suitable choice for the potential parameters was proposed by Ross and McMahan:[14] $\alpha=13$, $\epsilon/k_B=235$ K, and $r_m=4.47$ Å. Previous work has shown that this model allowed to reproduce accurately the phase diagram of xenon, both for the liquid-vapor transition and, more importantly for this work, for the solid-liquid and the solid-solid transitions.[15,16]

We focus on the high temperature–high pressure domain and study the entire crystallization process (nucleation and growth) under those conditions. We work at a supercooling of 25% (i.e., at a temperature 25% below the melting temperature) for two different pressures: $P=4.46$ GPa and $P=87.96$ GPa (the temperatures corresponding to a supercooling of 25% are, respectively, equal to $T=749.06$ K and $T=4406.25$ K). For a degree of supercooling of 25%, nucleation is an activated process.[3,4,18] The system has to overcome a large free energy barrier of nucleation to form a critical nucleus. In order to study this activated, or rare, event, we choose to perform hybrid Monte Carlo simulations together with the umbrella sampling technique.[3,19–21] The umbrella sampling technique is a non-Boltzmann sampling method in which a so-called umbrella bias potential is applied. The bias potential is a harmonic function of the global parameter Q_6, introduced by Steinhardt *et al.*[22] Q_6 gives a measure of the amount of crystalline order in the system studied. It is equal to 0 for a liquid and takes similar values for all the structures we will encounter in this work.[22] Therefore, applying a reaction coordinate such as Q_6 in the bias potential will not favor the formation of a specific polymorph over another.[5,8,7] Q_6 can be defined as follows:[3]

$$Q_6=\left[\frac{4\pi}{13}\sum_{m=-6}^{6}\left|\frac{\sum_i\sum_j Y_{6m}(\hat{\mathbf{r}}_{ij})\alpha(r_{ij})}{\sum_i\sum_j\alpha(r_{ij})}\right|^2\right]^{1/2}, \quad (2)$$

where $\mathbf{r}_{ij}$ is the vector joining two neighboring atoms (two atoms are considered as neighbors if they are separated by a distance r_{ij} smaller than a cutoff distance r_q, corresponding to the first minimum of the pair correlation function in the liquid phase), r_{ij} is its norm, $\hat{\mathbf{r}}_{ij}$ is the corresponding unit vector, $Y_{6m}(\hat{\mathbf{r}}_{ij})$ is a spherical harmonics, and $\alpha(r_{ij})$ a weight function, which goes smoothly to 0 to insure that Q_6 is a continuously differentiable function $[\alpha(r_{ij})=(r_{ij}-r_q)^2$ for $r_{ij}<r_q$ and $\alpha(r_{ij})=0$ elsewhere]. For $P=4.46$ GPa and $P=87.96$ GPa, we take $r_q=5.25$ Å and $r_q=4.25$ Å, respectively.

In this work, we combine the umbrella sampling technique with the hybrid Monte Carlo (HMC)[23–25] method introduced by Mehlig *et al.*[26] to study the nucleation event. All

the simulations are carried out in the *NPT* ensemble, i.e., at fixed number of atoms N, fixed temperature T, and fixed pressure P. There are two types of HMC steps. A HMC step is either a molecular dynamics trajectory of 20 time steps of 5 fs (67% of the HMC steps) or a Monte Carlo volume change (33% of the HMC steps—the amplitude of the volume change is adjusted in the course of the simulation so that 50% of these moves are accepted). Velocities are drawn from a Gaussian distribution at the beginning of each molecular dynamics trajectory. The Newtonian equations of motion are then integrated using a velocity-Verlet integrator. Once we have formed a critical nucleus, we study its spontaneous evolution in the absence of the bias potential. This allows us (i) to check that the critical nucleus we have formed is genuine and (ii) to analyze polymorph selection during the growth step. For this purpose, we embed the system of 3000 atoms containing the critical nucleus in a supercooled liquid matrix of 27 000 atoms and obtain a system containing a total of 30 000 atoms (we also carry out a couple of extended runs on systems of 50 000 atoms). We then equilibrate this system according to the following two successive steps. First, the central region of 3000 particles is frozen (i.e., kept fixed), and we let the rest of the system relax during a HMC simulation. Second, we carry out a HMC simulation of the whole system while applying the umbrella sampling bias potential to the central subsystem of 3000 particles. Every 500 HMC steps, we store an equilibrated configuration of the system (we repeat this procedure twenty times). Each of these twenty configurations will then be used as a starting point of an unbiased trajectory (i.e., with the bias potential switched off) in the *NPT* ensemble. Each unbiased trajectory is generated using a stochastic molecular dynamics simulation method, proposed by Attard,[27] for the isothermal-isobaric ensemble. This method consists of deterministic time steps (using Newton's equations of motion), alternated with stochastic steps based on the Boltzmann distribution (it is very similar to the popular method proposed by Andersen[28]). During each deterministic time step, we integrate the equation of motion with a velocity-Verlet integrator and a time step of 2 fs. We generate 20 unbiased evolutions of a critical nucleus. We observe the dissolution of the nucleus in the surrounding liquid for ten of them and the growth of the nucleus in the remaining ten free evolutions. The 1:1 ratio obtained demonstrates that the crystal nuclei we have formed are critical nuclei.

Throughout nucleation and growth, we need to identify the structural identity of each atom. In this work, we consider three different structures: fcc, hcp, or bcc. In order to carry out this analysis, we first need to compute the local order parameters q_6, q_4, and $\hat{w}_4$ for each atom[22] (in this calculation, we use a shorter cutoff distance to define pairs of neighboring particles: the cutoff distances are equal to 4.5 and 3.9 Å for $P=4.46$ GPa and $P=87.96$ GPa, respectively). We now briefly present how we proceed (this analysis is detailed in previous work[5,8,9]). Once we have computed the local order parameters, we need to identify which atoms are solidlike and which atoms are liquidlike. This is done according to the method proposed by ten Wolde *et al.*[3] on the basis of the amount of correlation between the local parameters of two neighboring molecules. When an atom is identified as solidlike, we then assign a structural identity to this atom, according to the value of q_4 and $\hat{w}_4$ for this atom, as shown in Fig. 2. An atom is identified as fcc-like if $q_4(i)>0.16$ and $w_4(i)<-0.05$, bcc-like if $q_4(i)<0.08$ or if $q_4(i)<0.11$ and $w_4(i)<-0.025$, and hcp-like if $q_4(i)>0.1$ and $w_4(i)>0.04$. These rules are summarized in Fig. 1. We use the same rules for the two state points studied. As shown in Fig. 2, we do not try to assign a specific structure to a particle where there is a significant overlap. This is because we prefer being positive on the structural identity of a given particle and leave the identity of some particles as undetermined. We find this analysis satisfactory since it allows us to identify 70% of the structure inside the crystal nucleus.

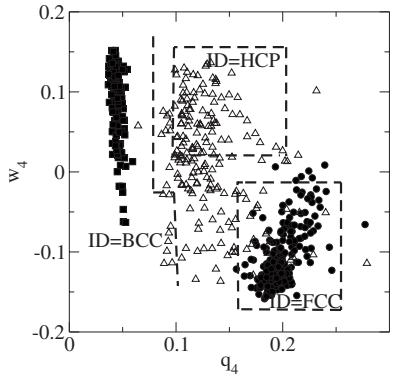

FIG. 2. Rules used to determine whether an atom is fcc-like, bcc-like, or hcp-like. Black filled squares, black filled circles, and triangles correspond to the values of $(q_4, \hat{w}_4)$ obtained for configurations of the bcc, fcc, and hcp crystals equilibrated at $T=749.06$ K and $P=4.46$ GPa.

III. RESULTS AND DISCUSSION

We first present the results obtained for the nucleation step. Using the umbrella sampling technique allows us to determine the properties of the critical nucleus, i.e., its size and structure, as well as the free energy barrier of nucleation. Snapshots of critical nucleus for the two sets of conditions studied, $P=4.46$ GPa and $P=87.96$ GPa for a supercooling of 25%, are shown in Fig. 3. The early stages of the nucleation step appear to be fairly insensitive to the thermodynamics conditions. For both pressures, nucleation starts with the formation of small bcc clusters. This is in agreement with the theoretical prediction of Alexander and McTague.[29] Using a Landau expansion for the free energy, Alexander and McTague[29] concluded that the bcc phase is favored during the nucleation for all simple fluids. This finding is also consistent with previous simulation studies on the crystallization of hard spheres,[30] of the Lennard-Jones fluid[3,5] or of charge-stabilized colloidal suspensions, modeled by the Yukawa potential.[7,8] However, as the precritical crystal nuclei grow and get closer to the critical size, the two systems follow two very different behaviors. We recall that at $P=4.46$ GPa, the bcc form is metastable while the fcc form is the thermodynamically stable phase.[15,16] At $P=4.46$ GPa, we observe that the metastable bcc-like atoms, present in the early stages of

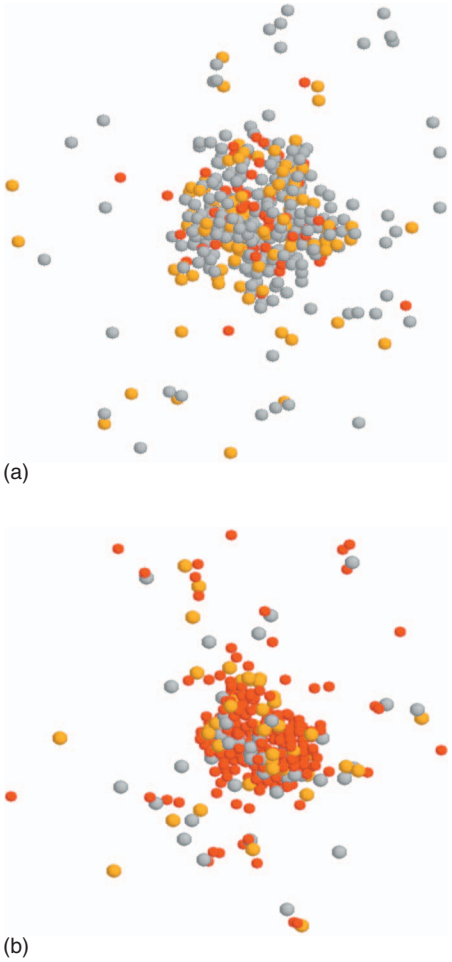

FIG. 3. (Color) Outside view of the critical nucleus for (a) $P=4.41$ GPa and (b) $P=87.96$ GPa. Gray: fcc; yellow: hcp; and red: bcc.

the nucleation, quickly turn into the stable fcc-like atoms as the size of the nucleus increases. This observation is consistent with the results obtained on the Lennard-Jones system at low pressures.[3,7] More generally, when fcc is the stable phase, this result confirms that it is only either in the late stages of the nucleation step, i.e., when the size of the crystal nucleus becomes close to the critical size (as in this case or in the case of the Lennard-Jones system at low pressure[3,7]), or during the growth step (as seen in the case of the Yukawa potential when the screening is large[8]) that the structure of the crystal nucleus becomes predominantly that of the stable phase. Finally, at the top of the free energy barrier (we estimate its height to be $35 \pm 2k_BT$), we obtain a critical nucleus composed of 195 ± 49 atoms. As shown in Fig. 3, the core is mainly composed of fcc-like atoms (60% of the atoms identified). The hcp-like and bcc-like atoms account for only 30% and 10%, respectively.

On the other hand, at $P=87.96$ GPa, nucleation starts and proceeds into the bcc phase. The bcc-like atoms remain predominant throughout the nucleation step and represent 50% of the identified atoms in the critical nucleus (see Fig 3), while the hcp-like and fcc-like atoms both account for 25%. The critical nucleus, composed of 296 ± 62 atoms, is larger

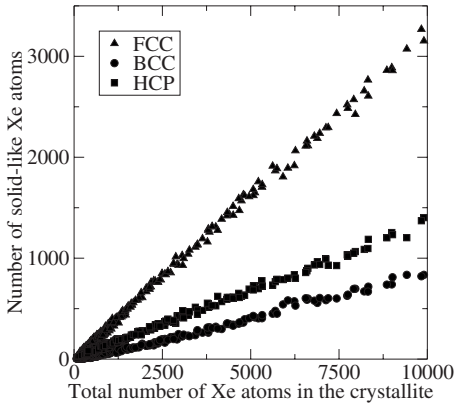

FIG. 4. Evolution of the number of fcc, bcc, and hcp atoms as a function of the total number of xe atoms in the crystallite for $P=4.41$ GPa.

than at $P=4.46$ GPa and the free energy barrier of nucleation, equals $20 \pm 2k_BT$, is lower than at $P=4.46$ GPa. The interpretation of this result is less straightforward than in the previous case. We recall that, for this pressure, the bcc form is the stable solid phase at the temperature of the solid-liquid transition and at low supercooling.[15,16] However, the conditions of crystallization used in this work, i.e., a supercooling of 25%, lie within the domain of stability of the fcc form (see Fig. 1). Therefore, at $P=87.96$ GPa, nucleation starts and proceeds in the bcc form, which is metastable at the chosen supercooling, rather than in the stable fcc phase as observed for $P=4.46$ GPa. What is the reason accounting for this difference? At $P=87.96$ GPa, the bcc form has a lower free energy than the liquid for all temperatures below the melting temperature. This implies that the conditions of crystallization lie within the domain of occurrence of the bcc form. The small precritical bcc clusters, which form at the beginning of the nucleation step, are thus more stable than the surrounding liquid and as such, continue to grow without, e.g., dissolving back into the liquid and rearranging into predominantly fcc clusters as observed at $P=4.46$ GPa. This mechanism is similar to that observed for the Lennard-Jones fluid[7] at high enough pressures, where nucleation proceeds entirely in the metastable bcc phase, or for Yukawa systems at small enough screening,[8,9] where nucleation also leads to the formation of critical nuclei, whose structure is predominantly that of the metastable bcc phase.

We now turn to the results obtained for the growth of the critical nuclei for the two sets of conditions. Throughout the growth of the crystallites, we monitor the evolution of the number of fcc-like, bcc-like, and hcp-like atoms. At $P=4.46$ GPa, all trajectories showed the same qualitative behavior. We plot in Fig. 4 the evolution (averaged over the 20 trajectories leading either to the growth or to the dissolution of the critical nuclei) of each type of atoms as a function of the total number of xenon atoms in the crystallite. A snapshot of a typical postcritical crystallite is also presented in Fig. 6(a). Figure 4 shows that the average number of fcc-like atoms increases at a much faster rate than that of hcp-like and bcc-like atoms. This simply corresponds to the fact that the postcritical crystallites are predominantly of the stable

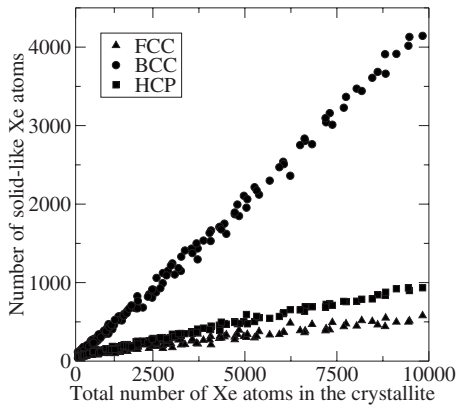

FIG. 5. Evolution of the number of fcc, bcc, and hcp atoms as a function of the total number of xe atoms in the crystallite for $P=87.96$ GPa.

fcc form, while bcc-like and hcp-like atoms appear mostly on the surface as defects. This is confirmed by the cross section of the crystallite presented in Fig. 6(a). While the evolution of each type of atoms as a function of the total number of atoms in the crystallite (Fig. 4) looks similar to that observed for the Lennard-Jones system at low pressure,[5,31] there is a significant difference between the crystallization mechanisms of the two systems. For the Lennard-Jones system at low pressure, we observed the formation of layers of the hcp form on the surface of the fcc nucleus, resulting from the cross nucleation (or heterogeneous nucleation) of the hcp form on the structurally compatible (111) planes of the fcc form as in the Lennard-Jones system.[5,31] However, we do not observe any cross-nucleation event during the crystallization of xenon at $P=4.46$ GPa. While we can notice the presence of small groups hcp-like atoms in the snapshots presented in Fig. 5, we did not observe the formation of hcp layers as for the Lennard-Jones system. The arrangement we observe here may be best described as a fcc crystal with hcp stacking faults. This is similar to the random packing structures of hcp-like and fcc-like atoms observed during the nucleation of hard spheres[30] or other very dense systems such as metals.[23,24]

At $P=87.96$ GPa, all growth trajectories lead to similar trends for the populations of each type of atoms. We plot in Fig. 5 the evolution, averaged over the 20 trajectories leading either to the growth or to the dissolution of the critical nuclei, of each type of atoms as a function of the total number of xenon atoms in the crystallite. Snapshots of typical postcritical crystallites are also presented in Fig. 6, obtained at the end of a growth trajectory for a system of 30 000 atoms [Fig. 6(b)] or at various stages of a growth trajectory for a system of 50 000 atoms [Figs. 6(c) and 6(d)]. Figure 5 shows that the number of bcc-like atoms increases faster than that of fcc-like and hcp-like atoms, indicating that the postcritical crystallites are predominantly of the stable bcc form. However, the growth mechanism is more complex than that observed at $P=4.46$ GPa. During the course of the growth of the postcritical crystallites, the crystallites can often be described as either monocrystalline [see Fig. 6(b)] or composed of two blocks: a large bcc block and a smaller fcc block [see,

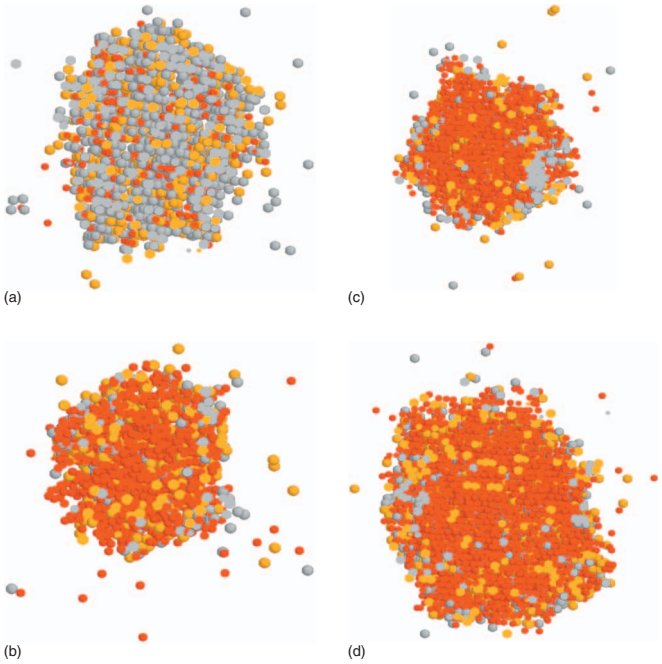

FIG. 6. (Color) Snapshots of typical large postcritical nuclei (a) at the end of a growth trajectory for a system of 30 000 atoms ($P=4.41$ GPa), (b), at the end of a growth trajectory for a system of 30 000 atoms ($P=87.96$ GPa), [(c) and (d)] or during the course of a growth trajectory for a system of 50 000 atoms ($P=87.96$ GPa). Same legend as in Fig. 3.

e.g., the fcc block on the right hand side of Fig. 6(d)] (hcp-like atoms are mostly scattered on the surface). The growth mechanism for the small fcc block can be described as follows. At some point during the growth step, a patch of fcc-like atoms forms on the surface of the bcc nucleus (instead of the more random scattering of fcc-like atoms observed in the majority of the cases) and grows to form a small fcc block. The fcc block grows at a much slower rate than the bcc block and thus slows down the growth of the crystallite. Later on during the growth, the fcc block converts into the bcc form [fcc blocks are absent from the snapshot of the crystallite, plotted in Fig. 6(d), taken at a later stage during the growth]. As discussed above, the formation and growth of the bcc block are kinetically favored. On the other hand, the existence of the fcc block is favored by thermodynamics, since fcc is the stable phase under the conditions of crystallization. Obtaining crystallites with two coexisting (at least for the time scales spanned during the simulation) fcc and bcc blocks is simply an illustration of the interplay between thermodynamics and kinetics. We finally add that it is rather unusual to obtain large crystallites composed of two blocks of different structures. For instance, we did not observe any in our simulations of the Lennard-Jones system. On the other hand, for the Yukawa systems with a large screening parameter,[8,9] we had already observed crystallites composed of a large fcc block (the stable phase in that case) and of a small metastable bcc block. However, there was a subtle difference with xenon since the small metastable bcc block, observed for the Yukawa system, had formed during the nucleation step, while the small stable fcc block, observed for xenon, forms during the growth step.

IV. CONCLUSIONS

In this work, we have simulated the entire crystallization process at high temperature and high pressure. We used two different simulation methods to simulate the two steps of the crystallization process, i.e., the nucleation and the growth steps. First, we combined the umbrella sampling technique with the hybrid Monte Carlo method to study the nucleation step and form a critical nucleus. We then performed a stochastic molecular dynamics simulation method to generate different evolutions of the critical nucleus and simulate the growth step. We chose two different conditions of pressure: $P=4.46$ GPa and $P=87.96$ GPa. In both cases, we worked at fixed supercooling, i.e., at a temperature 25% below the melting temperature. We have demonstrated that the crystallization mechanism dramatically depended on pressure. At $P=4.46$ GPa, both crystal nucleation (with the exception of the very early stages) and growth proceeded through the stable fcc polymorph. We found that the crystallization mechanism departed from that of the Lennard-Jones system since we did not observe any cross nucleation. Instead, we observed a random packing of fcc-like and hcp-like atoms as seen for hard spheres or very dense systems (metals) for which fcc is also the stable form. At $P=87.96$ GPa, our simulations revealed that, throughout the crystallization process, the crystallites were always predominantly of the bcc form, which is the stable crystalline form at the solid-liquid transition but is metastable at a supercooling of 25%. We observed the formation of crystallites composed of two blocks: a large block of the bcc polymorph and a smaller and transient block of the fcc polymorph. The existence of the large bcc block was justified in terms of kinetics as the conditions of crystallization lie within the domain of occurrence of the bcc form (i.e., the domain in which bcc is more stable than the liquid). We noted some similarities with our previous work on the Yukawa systems, in which we found crystallites with coexisting fcc and bcc blocks. The existence of the smaller fcc block, formed during the growth step, was found to arise from the thermodynamic stability of the fcc form. The crystallization mechanism of xenon was again found to depart from that of the Lennard-Jones system since no large coexisting blocks of fcc and bcc have been observed so far during the crystallization of the Lennard-Jones system.

[1] J. Bernstein, *Polymorphism in Molecular Crystals* (Oxford University Press, Oxford, 2002).
[2] J. Bernstein, R. J. Davey, and J. O. Henck, Angew. Chem., Int. Ed. **38**, 3441 (1999).
[3] P. R. ten Wolde, M. J. Ruiz-Montero, and D. Frenkel, Phys. Rev. Lett. **75**, 2714 (1995).
[4] F. Trudu, D. Donadio, and M. Parrinello, Phys. Rev. Lett. **97**, 105701 (2006).
[5] C. Desgranges and J. Delhommelle, J. Am. Chem. Soc. **128**, 10368 (2006).
[6] M. S. G. Razul, J. G. Hendry, and P. G. Kusalik, J. Chem. Phys. **123**, 204722 (2005).
[7] C. Desgranges and J. Delhommelle, Phys. Rev. Lett. **98**, 235502 (2007).
[8] C. Desgranges and J. Delhommelle, J. Am. Chem. Soc. **128**, 15104 (2006).
[9] C. Desgranges and J. Delhommelle, J. Chem. Phys. **126**, 054501 (2007).
[10] T. Goto, Y. Nakata, and S. Morita, Anesthesiology **98**, 1 (2003).
[11] J. L. Brown, D. A. Glaser, and M. L. Perl, Phys. Rev. **102**, 586 (1956).
[12] M. W. Rowe, D. D. Boggard, C. E. Brothers, and P. K. Kuroda, Phys. Rev. Lett. **15**, 843 (1965).
[13] R. A. Buckingham,Proc. R. Soc. London, Ser. A **168**, 264 (1938).
[14] M. Ross and A. K. McMahan, Phys. Rev. B **21**, 1658 (1980).
[15] F. Saija and S. Prestipino, Phys. Rev. B **72**, 024113 (2005).
[16] A. B. Belonoshko, S. Davis, A. Rosengren, R. Ahuja, B. Johansson, S. I. Simak, L. Burakovsky, and D. L. Preston, Phys. Rev. B **74**, 054114 (2006).
[17] S. Prestipino, F. Saija, and P. V. Giaquinta, J. Chem. Phys. **123**, 144110 (2005).
[18] P. R. ten Wolde, M. J. Ruiz-Montero, and D. Frenkel, J. Chem. Phys. **104**, 9932 (1996).
[19] G. M. Torrie and J. P. Valleau, Chem. Phys. Lett. **28**, 578 (1974).
[20] J.-M. Leyssale, J. Delhommelle, and C. Millot, J. Am. Chem. Soc. **126**, 12286 (2004).
[21] J.-M. Leyssale, J. Delhommelle, and C. Millot, J. Chem. Phys. **122**, 104510 (2005).
[22] P. J. Steinhardt, D. R. Nelson, and M. Ronchetti, Phys. Rev. B **28**, 784 (1983).
[23] C. Desgranges and J. Delhommelle, J. Am. Chem. Soc. **129**, 7012 (2007).
[24] C. Desgranges and J. Delhommelle, J. Chem. Phys. **127**, 144509 (2007).
[25] C. Desgranges and J. Delhommelle, J. Phys. Chem. B **111**, 12257 (2007).
[26] B. Mehlig, D. W. Heermann, and B. M. Forrest, Phys. Rev. B **45**, 679 (1992).
[27] P. Attard, J. Chem. Phys. **116**, 9616 (2002).
[28] H. C. Andersen, J. Chem. Phys. **72**, 2384 (1980).
[29] S. Alexander and J. P. McTague, Phys. Rev. Lett. **41**, 702 (1978).
[30] S. Auer and D. Frenkel, J. Phys.: Condens. Matter **3**, 873 (2003).
[31] C. Desgranges and J. Delhommelle, J. Phys. Chem. B **111**, 1465 (2007).